

# Highlighting protein kinase CK2 movement in living cells

Nathalie Theis-Febvre,<sup>1</sup> Véronique Martel,<sup>1</sup> Béatrice Laudet,<sup>1</sup>  
Catherine Souchier,<sup>2</sup> Didier Grunwald,<sup>3</sup> Claude Cochet<sup>1</sup>  
and Odile Filhol<sup>1</sup>

<sup>1</sup>INSERM EMI 104, Département Réponse et Dynamique Cellulaires, CEA 38054, Grenoble, France; <sup>2</sup>INSERM U309, Institut Albert Bonniot, 38706 La Tronche, France; <sup>3</sup>INSERM EMI 9931, Département Réponse et Dynamique Cellulaires, CEA 38054 Grenoble, France

## Abstract

Protein kinase CK2 has traditionally been described as a stable heterotetrameric complex ( $\alpha_2\beta_2$ ) but new approaches that effectively capture the dynamic behavior of proteins, are bringing a new picture of this complex into focus. To track the spatio-temporal dynamics of CK2 in living cells, we fused its catalytic  $\alpha$  and regulatory  $\beta$  subunits with GFP and analog proteins. Beside the mostly nuclear localization of both subunits, and the identification of specific domains on each subunit that triggers their localization, the most significant finding was that the association of both CK2 subunits in a stable tetrameric holoenzyme eliminates their nuclear import (Mol Cell Biol 23: 975–987, 2003). Molecular movements of both subunits in the cytoplasm and in the nucleus were analyzed using different new and updated fluorescence imaging methods such as: fluorescence recovery after photo bleaching (FRAP), fluorescence loss in photo bleaching (FLIP), fluorescence correlation spectroscopy (FCS), and photoactivation using a biphoton microscope. These fluorescence-imaging techniques provide unprecedented ways to visualize and quantify the mobility of each individual CK2 subunit with high spatial and temporal resolution. Visualization of CK2 heterotetrameric complex formation could also be recorded using the fluorescence resonance energy transfer (FRET) technique. FRET imaging revealed that the assembling of this molecular complex can take place both in the cytoplasmic and nuclear compartments. The spatio-temporal organization of individual CK2 subunits and their dynamic behavior remain now to be correlated with the functioning of this kinase in the complex environment of the cell. (Mol Cell Biochem 274: 15–22, 2005)

*Key words:* protein kinase CK2, localization, targeting, movement, subunit interaction

## Introduction

Protein kinase CK2 is a pleiotropic and almost universal protein kinase that has crucial roles in cell differentiation, proliferation and survival [2, 3]. Many of the identified CK2 substrates that are critical for cell proliferation and viability are localized in different cell compartments. It is, therefore, suspected that targeting CK2 to specific sub-cellular loca-

tions is crucial to many of its roles. Although the common view describes this enzyme as a tetrameric complex consisting of two  $\alpha$  catalytic subunits and two  $\beta$  regulatory subunits, accumulating evidence indicate that free populations of both CK2 subunits can exist and exert specific functions in the cell [1, 4, 5]. Sub-cellular localization and targeting of protein kinases play important roles in signal transduction that regulates many cellular processes. Thus, understanding

how a multifunctional enzyme like CK2 can achieve specificity of action over time and space requires an understanding of both the localization and the functional interaction of its subunits. Due to the advent of fluorescent protein technology, it has been feasible to visualize, track and quantify molecules and events in living cells [6, 7].

In the current work, we have applied recent fluorescent microscopy imaging techniques to monitor the localization and trafficking of the CK2 subunits and their interaction in the complex environment of a cell.

## Materials and methods

### *Constructs of plasmids encoding photoactivatable GFP-CK2 subunits*

The cDNA encoding CK2 $\alpha$  and CK2 $\beta$  were sub-cloned from EGFP-CK2 $\alpha$  or  $\beta$  [1] into PA-GFPc1 plasmid [8].

### *Transient transfection of NIH 3T3 cells*

NIH 3T3 cells were transiently co-transfected using Fugene 6 reagent (Roche) according to the manufacturer's instructions, with PA-GFP, PA-GFP CK2 $\alpha$  or PA-GFP CK2 $\beta$  together with DsRED-N1 plasmid (ratio 1/2) to visualize the transfected cells before photoactivation. One day after transfection, the cell medium was changed to remove the pH indicator phenol red and 10 mM HEPES was added to DMEM supplemented with 10% fetal calf serum (FCS) to buffer it.

### *Photo-activation*

Activation of GFP fluorescence either in the nucleus or in the cytoplasm was performed using a biphoton microscope (LSM510-NLO, Zeiss) at the 720 nm wavelength in a small area (circle 30  $\times$  30 pixels) using 10 iterations with 50% of the maximum laser power (fs Ti: Sa Tsunami, Spectra Physics). Photo-activated GFP images were then acquired at 488 nm using argon laser.

Control experiments showed that bleaching of the PA-GFP (photoactivatable GFP) during imaging was not detected. An image of the entire cell before and after photoactivation was recorded.

### *Nuclear import measurement*

Typically, PA-GFP containing cells were detected via DsRed expression. PA-GFP proteins were photoactivated inside the cytoplasm, in different spots (at least three) during 1 min max-

imum and immediately after, an image of the entire cell was recorded every 60 s during 15 min. The fluorescence intensity in both nucleus and cytoplasm was measured and the ration of these intensities minus the initial intensity was plotted over time. Three PA-GFP CK2 $\alpha$ , four PA-GFP CK2 $\beta$  and two PA-GFP control-expressing cells were monitored in three independent experiments.

### *Measurement of PA-GFP CK2 subunits mobility*

NIH 3T3 fibroblasts transiently expressing PA-GFP CK2 subunits were submitted to a "visible pulse chase experiment": photoactivation was performed in a tiny region of interest (ROI) (30  $\times$  30 pixels) either in the cytoplasm or in the nucleus, and immediately after, the fluorescent signal was followed in a time series (every 62 ms) for  $\sim$ 3 min, to follow the PA-GFP. Fluorescence intensity was plotted over time, and the resulting curves were fitted using Origin Software with an exponential decay function:  $y = a_1 \exp(-x/t_1) + a_2 \exp(-x/t_2) + y_0$ .

### *Labeling of CK2 $\beta$ with Cy3*

Recombinant CK2 $\beta$  was labeled with Cy3 as recommended by the manufacturer (Amersham Kit PA23001): 200  $\mu$ g of bacterially expressed CK2 $\beta$  were equilibrated in 0.1 M Na Carbonate pH 9.3 and added to the labeling kit for 30 min at 22  $^{\circ}$ C. To remove the unbound Cy3, the reaction was loaded on a G50 gel filtration column equilibrated in PBS and concentrated in a Vivaspin micro concentrator (cutoff 30 kDa, Vivascience).

### *Microinjection*

NIH 3T3 mouse fibroblasts stably expressing GFP, GFP CK2 $\alpha$  or GFP CK2 $\beta$  [1] were grown at 37  $^{\circ}$ C in Dulbecco's modified Eagle's medium (DMEM) supplemented with 10% (v/v) FCS in 5% CO $_2$  atmosphere. Prior to microinjection, the cells were placed on medium supplemented with 10 mM HEPES-pH 7.4, and the solution containing Cy3-labeled CK2 $\beta$  was centrifuged for 15 min at 1,00,000 g in a TL100 Beckman Airfuge. NIH 3T3 cells were microinjected using a semiautomatic micro injector (Eppendorf). After injection, the cells were allowed to recover for one hour at 37  $^{\circ}$ C in 5% CO $_2$  atmosphere before fixation with 4% Para formaldehyde for 20 min.

### *FRET imaging*

Fluorescence images of fixed cells were acquired on a confocal laser-scanning microscope (LEICA TCS-SP2). GFP

and Cy3 were excited with the 488 nm wavelength of an argon laser and a 543 nm wavelength of an He/Ne laser respectively. FRET was determined by the acceptor photo bleaching method according to the following sequence: (i) a pre-photo bleach GFP (donor) image was acquired by scanning with 488 nm light; (ii) an intracellular ROI was selected and rendered free of Cy3 (acceptor) by repeated scanning with the 543 nm laser ray until all Cy3 was photo destructed; (iii) a post-photo bleach GFP image was acquired by scanning with a 488 nm laser; (iv) the FRET efficiencies in the ROI were calculated from image subtraction between the two (post-bleach and pre-bleach) GFP images.

## Results

### *Nuclear import kinetics of CK2 subunits*

Previous results have shown that both CK2 subunits contain nuclear localization domains that target them independently to the nucleus. However, for technical reasons, the dynamic of the GFP-CK2 $\beta$  nuclear import could not be analyzed in this study [1]. To go further in this direction, we took advantage of the recently developed photoactivatable fluorescent protein, PA-GFP [9]. This protein displays little fluorescence under excitation at the imaging wavelength (488 nm) but exhibits up to 100-fold increase in fluorescence after irradiation at a different wavelength. Both CK2 subunits were cloned into the PA-GFP plasmid and expressed in NIH 3T3 fibroblasts. To highlight and follow the fate of PA-GFP proteins in living cells, we selectively photoactivated a subpopulation of PA-GFP CK2 subunits in the cytoplasmic compartment of expressing cells and observed their behaviors over time (Fig. 1). The photoactivation was efficiently performed using a biphoton excitation at 720 nm, illustrating a new application of multiphoton fluorescence microscopy. After  $\sim 1$  s of photoactivation within different spots in the cytoplasm (determined by Nomarski imaging), the cytoplasmic pool of PA-GFP CK2 subunits became highly fluorescent under 488 nm excitation and the fluorescent signal appeared relatively homogeneous. This observation suggests a high mobility of the photoactivated molecules inside this cell compartment (Fig. 1A a, a', a''). Continued imaging with 488 nm light revealed rapid movement of the photoactivated GFP alone, across the nuclear envelope, and into the nucleus, resulting in its equilibration throughout the cell in a matter of 5 min (Fig. 1A a, b, c, d and B) as previously described [8]. For PA-GFP-CK2 $\alpha$ , the nuclear translocation was less rapid than for PA-GFP alone, as shown in Fig. 1A a', b', c', d' and B. The equilibration of the fluorescence signal throughout the cell was only detectable after 15 min. In contrast, during this

time frame, the nuclear translocation of PA-GFP-CK2 $\beta$  was barely detectable (Fig. 1A a'', b'', c'', d'' and B). Panel B in Fig. 1 represents the ratio of fluorescence intensity normalized by the fluorescence intensity at  $t = 0$ , for several types of PA-GFP-molecule expressing cells measured both in the nucleus and in the cytoplasm. Altogether, these experiments show that the nuclear import kinetics of CK2 subunits are different, CK2 $\beta$  being the less rapid in this translocation. The fact that CK2 $\alpha$  is slower than GFP alone agrees for an active transport of this kinase subunit as compare to the passive diffusion of PA-GFP.

### *Mobility of PA-GFP-CK2 subunits in living cells*

In our previous study, the FLIP technique clearly showed that GFP-CK2 $\alpha$  moves faster than GFP-CK2 $\beta$  both in the cytoplasm and in the nucleus [1]. A fluorescent correlation spectroscopy (FCS) approach revealed that both CK2 subunits could be separated in two subpopulations: one of fast moving CK2 subunits displaying diffusion constants similar to that of GFP and an-other subpopulation of slow moving CK2 subunits. This last population was characterized as CK2 subunits that are highly restricted in their mobility suggesting that they might be associated with less mobile structures in high molecular complexes. However, in contrast to the FLIP experiments, the FCS analysis did not indicate that in the fast moving population CK2 $\alpha$  and CK2 $\beta$  were diffusing at different rates. For this reason, we choose a third approach using PA-GFP photoactivation in a "visible pulse chase," to study the mobility of both CK2 subunits. A short pulse of activating light (720 nm with the biphoton excitation) confined only to one compartment of the cell (cytoplasm or nucleus) labeled the CK2 subunits expressed in this location. This generated an initial pool of fluorescent CK2 subunits that owing to their respective mobility diffused away from this region in all directions. The extent and rate at which this occurs can be quantified and used with computer-modeling approaches to describe the kinetic parameters of the protein. Measurements of fluorescence in the area in which CK2 subunits moved over time (Fig. 2) were performed both in the cytoplasm and in the nucleus. A typical graph is shown in Fig. 2 for each PA-GFP expressing cell type, after photoactivation inside the nucleus. The fluorescence decrease observed after the photoactivation step was fitted using a bi-exponential decay model. The main characteristic times are reported in Table 1. These results show that (i) there is no significant difference in the mobility of the three proteins in the nucleus as compared to the cytoplasm, (ii) the diffusion time for PA-GFP ( $0.66 \pm 0.06 \mu\text{s}$ ) is significantly shorter than that of the PA-GFP-CK2 subunits ( $> \mu\text{s}$ ) confirming that CK2 subunits are less mobile than GFP alone. However, this technical approach does

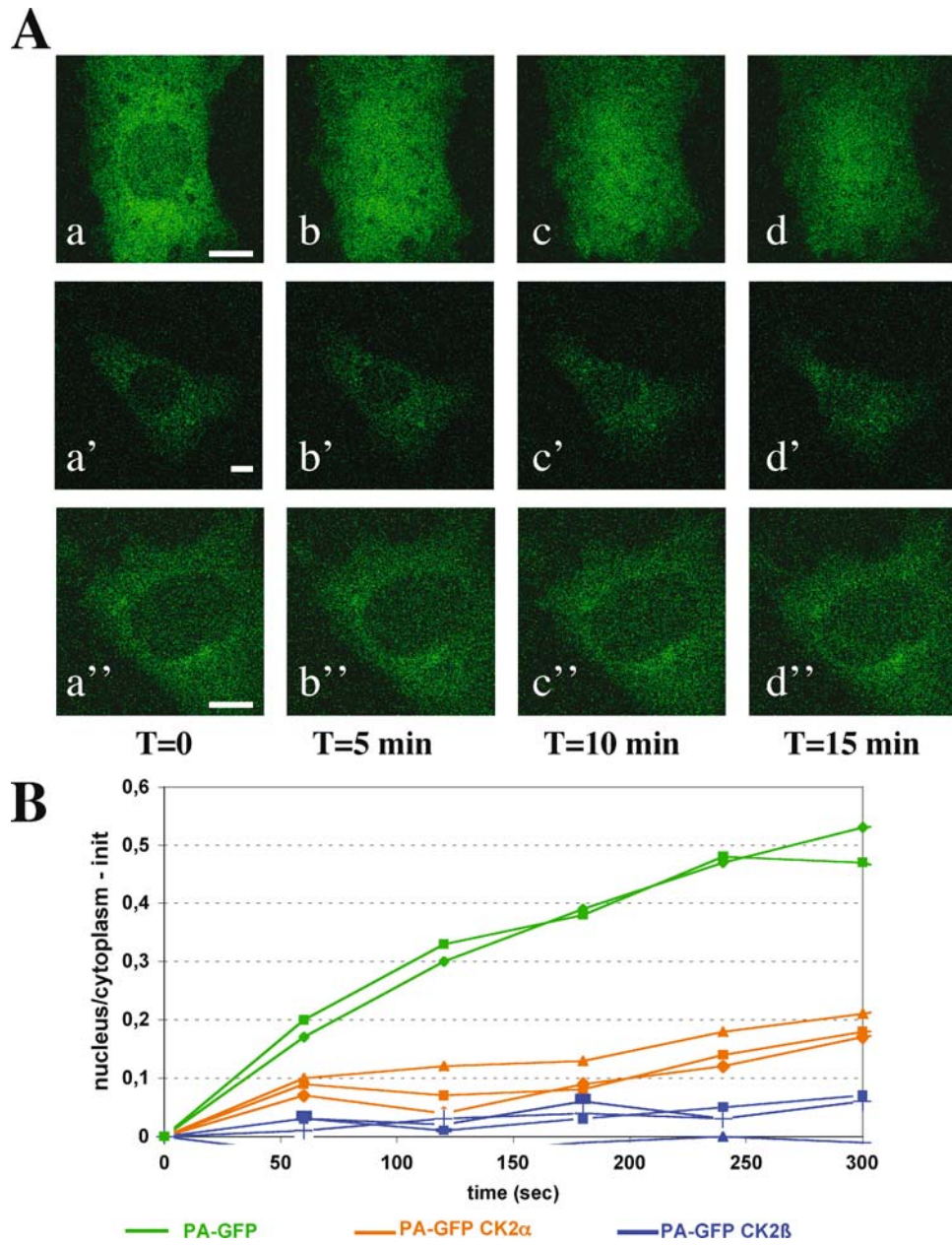


*Fig. 1.* Nuclear import of PA-GFP CK2 subunits. NIH 3T3 cells transiently transfected with either PA-GFP (a–d), PA-GFP-CK2 $\alpha$  (a'–d') or PA-GFP-CK2 $\beta$  (a''–d'') were photoactivated by illuminating inside the cytoplasm as described in Materials and methods section. Immediately after photoactivation, images of the whole cell were recorded every minute for 15 min. (A) Indicated time points are illustrated for each PA-GFP fusion proteins. Bar, 5  $\mu$ m. (B) The ratio of fluorescence intensity between the nucleus and the cytoplasm recorded in the three types of cells was plotted over time.

not provide evidence for a difference in mobility between CK2 subunits as previously observed by FLIP experiments [1].

However, the demonstration within the cell of a subtle equilibrium between the different forms of CK2 subunits raises the question of the reality of their functional interaction in living cells [5].

#### *Interaction of CK2 subunits visualized by in situ FRET experiments*

To visualize the interaction of CK2 subunits in a cell environment, we used *in situ* FRET experiments. After microinjection of Cy3-CK2 $\beta$ , cells were fixed and processed as described under Materials

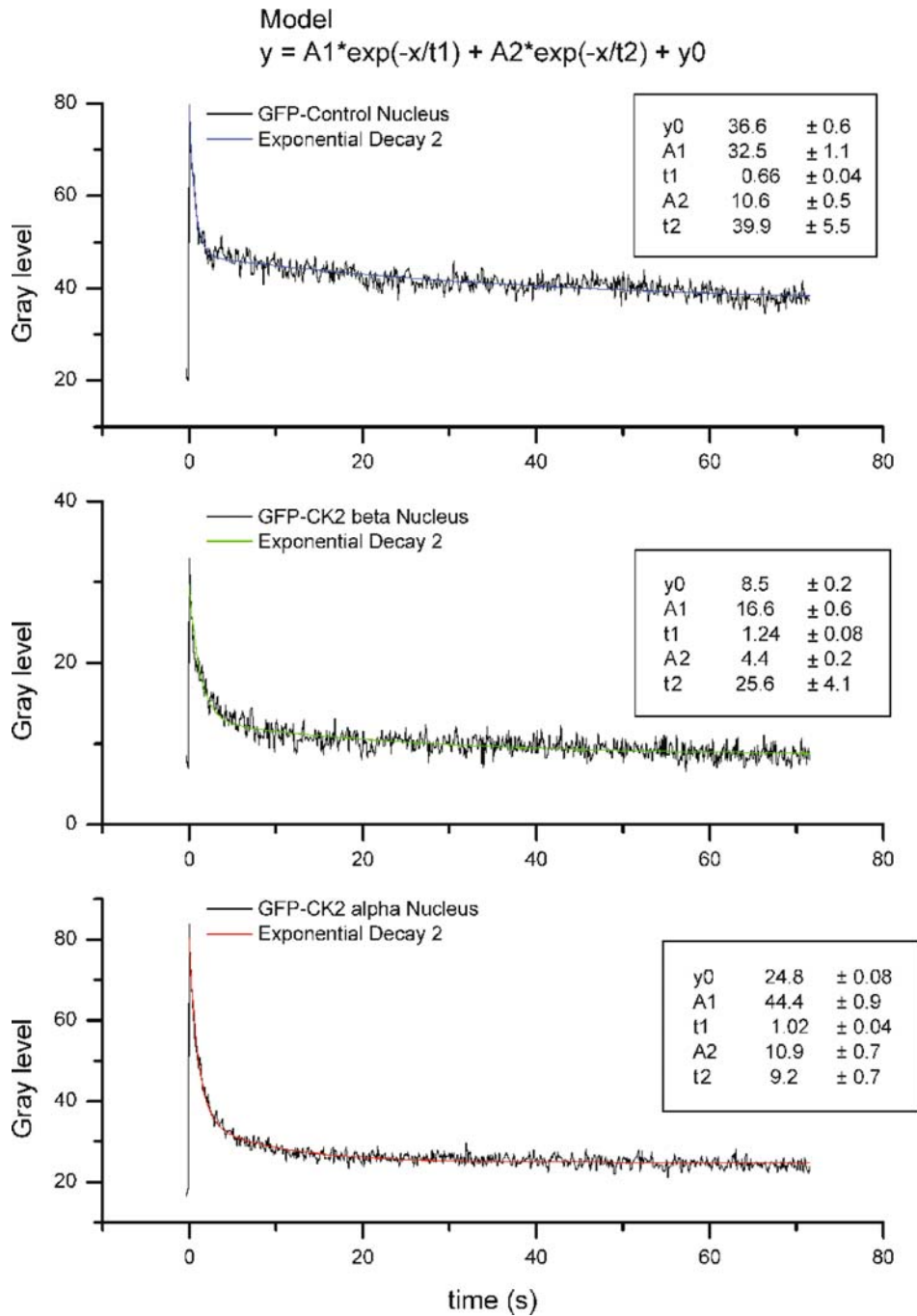


*Fig. 2.* Photo activation of PA-GFP CK2 subunits in living cells. NIH 3T3 cells transiently expressing PA-GFP, PA-GFP-CK2 $\alpha$  or PA-GFP-CK2 $\beta$  were photoactivated using a biphoton microscope in a small spot, either in the nucleus or in the cytoplasm. The fluorescent signal was then followed in a time series every 62 ms (600 images) inside the spot. A representative experiment is shown for PA-GFP, PA-GFP-CK2 $\alpha$  and PA-GFP-CK2 $\beta$  photoactivated inside the nucleus. Gray level corresponding to fluorescence intensity was plotted over time. Using Origin software, the curve was fitted with the exponential decay model.

and Methods, for acceptor photo bleaching FRET microscopy.

GFP-CK2 $\alpha$  expressing NIH 3T3 cells were microinjected with Cy3-CK2 $\beta$  in the cytoplasm and the corresponding

FRET efficiencies were determined (Fig. 3A). The first acquired image (D1) represents the fluorescence intensity distribution of the donor GFP-CK2 $\alpha$  directly excited at 488 nm. The second image (A1) represents the fluorescence intensity

Table 1. Photoactivation experiment

Cell	Localization	<i>N</i>	<i>t1</i> ( $\mu$ s)	<i>t1</i>
GFP <sup>b</sup>	Nucleus	9	$0.66 \pm 0.06^a$	$0.66 \pm 0.06^b$
	Cytoplasm	10	$0.66 \pm 0.11$	
GFP-CK2 $\alpha$	Nucleus	28	$1.04 \pm 0.10$	$1.02 \pm 0.06$
	Cytoplasm	20	$0.99 \pm 0.06$	
GFP-CK2 $\beta$	Nucleus	8	$1.20 \pm 0.10$	$1.33 \pm 0.11$
	Cytoplasm	10	$1.44 \pm 0.18$	

<sup>a</sup>Mean  $\pm$  S.E.M., *t1* value of the exponential model.

<sup>b</sup>Kruskal Wallis rank test, significant differences between GFP fusion proteins.

distribution of the acceptor Cy3-CK2 $\beta$  excited at 543 nm. The acceptor fluorophore was subsequently photo bleached in a define area of the field (demarcated by a white rectangle in A2 and D2) by repeated scanning with a 543 nm laser ray, thereby abolishing FRET. A second donor fluorescence image (D2) was obtained with 488 nm excitation. An increase of donor fluorescence intensity in the region of acceptor photo bleaching, would be expected only in cellular structures exhibiting FRET. Indeed, a brighter signal from the donor GFP-CK2 $\alpha$  was apparent in the cytoplasm containing Cy3-CK2 $\beta$ , indicating the existence of a complex between GFP-CK2 $\alpha$  and Cy3-CK2 $\beta$  in this cell compartment. The FRET efficiency throughout the cell was calculated by a simple image arithmetic operation (Fig. 3A, FRET [D2-D1]). As expected, the FRET signal outside the white rectangle was near zero.

The same technique was used to investigate the interaction of different GFP-tagged proteins with Cy3-CK2 $\beta$  (Fig. 3B). Column 1 (D1) depicts the donor (GFP, GFP-CK2 $\alpha$ , GFP-CK2 $\beta$ ) fluorescence intensity distribution in the cells, and column 2 (A1) the microinjected Cy3-CK2 $\beta$  signal; the white rectangle denotes the location of the acceptor free region after Cy3 photo destruction. The FRET efficiencies were calculated by subtraction of the donor fluorescence intensity images after and before Cy3 photo destruction (Fig. 3B, column 3, D2-D1). FRET was negligible in GFP expressing cells, but clearly detectable in the nucleus and to a lower extent in the cytoplasm of CK2 $\alpha$  and CK2 $\beta$  expressing cells, (compare Fig. 3B, FRET D2-D1 and Fig. 3A, FRET D2-D1). From these observations, we conclude that specific populations of CK2 $\alpha$  and CK2 $\beta$  are in close molecular proximity. The range over which FRET between a donor (GFP) and an acceptor (Cy3) fluorescent molecule varies in a sensitive manner is dictated by  $R_0$  (the distance at which the FRET efficiency is 50%).  $R_0$  for GFP/Cy3 system is between 2 and 6 nm [10]. Because no FRET signal could be detected with GFP alone, the observed FRET signals represent the interaction between Cy3-CK2 $\beta$  and CK2 $\alpha$  or CK2 $\beta$

respectively (Fig. 3). Unexpectedly, the FRET signal observed in cells expressing Cy3-CK2 $\beta$  and GFP-CK2 $\beta$  suggests that these two proteins are also in close molecular proximity. This homologous interaction between CK2 $\beta$  subunits can take place both in the nucleus and to a lesser extent, in the cytoplasm.

## Discussion

In this study we describe experiments aimed at going further into dynamic aspects of CK2 in living cells, focusing on three points: (i) comparison of both CK2 subunits nuclear import, (ii) intrinsic mobility using photoactivatable-GFP fused to CK2 subunits and (iii) *in situ* visualization of the subunit interaction by the FRET technology. Using the recently developed photoactivatable GFP proteins [9], we could show that GFP-CK2 $\beta$  enters into the nucleus much slower than GFP-CK2 $\alpha$ . This is in agreement with the idea that the nuclear import of both subunits is mediated by independent mechanisms. CK2 $\alpha$  contains in its sequence a classical NLS motif that is absent in CK2 $\beta$ . The rate of the regulatory subunit nuclear import is conceivable with the hypothesis that CK2 $\beta$  may “piggy pack” its way into the nucleus [11]. The FLIP and the FCS analysis showed that CK2 subunits are highly mobile. In addition, a differential kinetic behavior of each subunit was revealed by the FLIP analysis [1]. Using the photoactivation technique as a third independent approach, we have determined that the diffusion coefficients for each CK2 subunit fall into the same range of measurements. However, the resolution of the photoactivation technique and perhaps, the lack of enough cell number analyzed do not reveal a statistical difference in the kinetic behavior of each CK2 subunit. It is noteworthy that the FLIP and photoactivation techniques give access to results that represent the sum of movement of CK2 subunits in all their forms: activated, inactivated, free, bound, or bound to different partners. FCS analysis suggested the existence in living cells of two subpopulations of fast and slow moving CK2 subunits that could represent on one hand, the highly mobile free CK2, and on the other hand, less mobile CK2 subunit-containing macromolecular complexes. These observations also revealed that the CK2 subunits are not permanently associated, as previously thought, and that their molecular interaction is in fact highly dynamic.

*In situ* visualization of this molecular interaction could be demonstrated via the ectopically targeted expression of the CK2 $\beta$  to the plasma membrane [12]. These observations are strengthened by our FRET experiments that clearly demonstrate that in living cells, Cy3-CK2 $\beta$  interacts both with CK2 $\alpha$  and CK2 $\beta$ . X-ray crystallographic studies revealed that CK2 $\beta$  is a dimeric protein [13]. In the holoenzyme, two CK2 $\alpha$  that are not in contact with each other interact with a

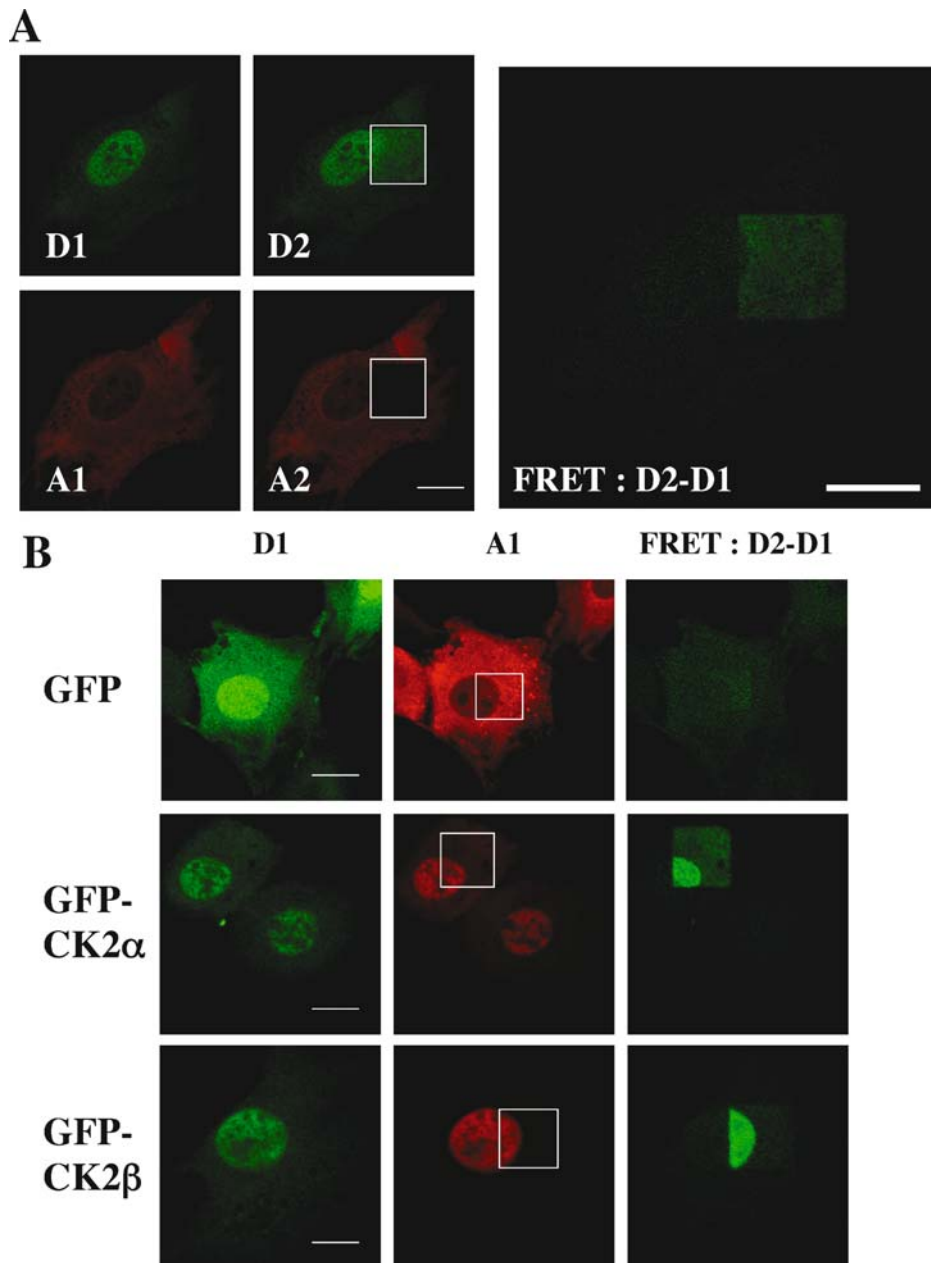


*Fig. 3.* Detection of molecular interaction between CK2 subunits by acceptor photo bleaching FRET microscopy. NIH 3T3 mouse fibroblasts stably expressing GFP, GFP-CK2 $\alpha$  or GFP-CK2 $\beta$  were microinjected with Cy3-CK2 $\beta$ . (A) Sequence of events to obtain FRET signal from acceptor photobleaching. A donor image D1 (GFP-CK2 $\alpha$  expressing cell) and an acceptor image A1 (Cy3-CK2 $\beta$ ) are acquired. The acceptor is photo bleached in a specific area of the cell by continuous scanning with the 543 nm laser line (A2). The intracellular reference regions created by Cy3 photo destruction are enclosed in white rectangles. After photo destruction of Cy3 a second donor image D2 is obtained. The FRET signal is shown in the difference image (D2-D1). (B) Vertical column from left to right: Column 1, fluorescence of stably GFP fusion proteins expressing cells indicated on the left (donor before bleaching = D1); Column 2, fluorescence of microinjected Cy3-CK2 $\beta$  (acceptor before bleaching = A1). The region in which the acceptor was photo bleached is marked with a white rectangle. Column 3, FRET signal calculated from the subtraction of post- and pre-Cy3 photo bleaching donor fluorescence images.

central building block that is represented by the CK2 $\beta$  dimer [14]. Since it is assumed that both Cy3-CK2 $\beta$  and GFP-CK2 $\beta$  are dimeric proteins [1, 13], the increase in fluorescence of the donor GFP-CK2 $\beta$  in FRET experiments could either reflect the incorporation of CK2 $\beta$  in high-order structure of the CK2

holoenzyme [15, 16], or the dynamic association/dissociation of the CK2 $\beta$  dimer.

Sub-cellular localization and targeting of protein kinases is a common theme in signal transduction. The sub-cellular dynamics of the CK2 subunits and the transient nature of

their interaction are the hallmarks of intracellular signaling molecules [3]. Our observations strengthen the notion that the regulation of CK2 activity must be understood within this context. Further studies are now required to correlate this complex dynamic with the functioning of this kinase in the cell environment.

## Acknowledgments

We thank Jacques Mezzega for the biphoton experiments. This work was supported by grants from the Institut National de la Santé Et de la Recherche Médicale (INSERM), the Commissariat à l'Energie Atomique and the Ligue Nationale contre le Cancer (équipe labellisée).

## References

1. Filhol O, Nueda A, Martel V, Gerber-Scokaert D, Benitez MJ, Souchier C, Saoudi Y, Cochet C: Live-cell fluorescence imaging reveals the dynamics of protein kinase CK2 individual subunits. *Mol Cell Biol* 23: 975–987, 2003
2. Ahmed K, Gerber DA, Cochet C: Joining the cell survival squad: An emerging role for protein kinase CK2. *Trends Cell Biol* 12: 226–230, 2002
3. Litchfield DW: Protein kinase CK2: Structure, regulation and role in cellular decisions of life and death. *Biochem J* 369: 1–15, 2003
4. Guerra B, Siemer S, Boldyreff B, Issinger OG: Protein kinase CK2: evidence for a protein kinase CK2beta subunit fraction, devoid of the catalytic CK2alpha subunit, in mouse brain and testicles. *FEBS Lett* 462: 353–357, 1999
5. Filhol O, Martiel JL, Cochet C: Protein kinase CK2: A new view of an old molecular complex. *EMBO Rep* 5: 351–355, 2004
6. Lippincott-Schwartz J, Patterson GH: Development and use of fluorescent protein markers in living cells. *Science* 300: 87–91, 2003
7. van Roessel P, Brand AH: Imaging into the future: Visualizing gene expression and protein interactions with fluorescent proteins. *Nat Cell Biol* 4: E15–E20, 2002
8. Patterson GH, Lippincott-Schwartz J: A photoactivatable GFP for selective photolabeling of proteins and cells. *Science* 297: 1873–1877, 2002
9. Patterson GH, Lippincott-Schwartz J: Selective photolabeling of proteins using photoactivatable GFP. *Methods* 32: 445–450, 2004
10. Wouters FS, Bastiaens PI, Wirtz KW, Jovin TM, Bastiaens PH, Wanders RJ, Seedorf U: FRET microscopy demonstrates molecular association of non-specific lipid transfer protein (nsL-TP) with fatty acid oxidation enzymes in peroxisomes. The non-specific lipid transfer protein (sterol carrier protein 2) acts as a peroxisomal fatty acyl-CoA binding protein. *EMBO J* 17: 7179–7189, 1998
11. Martel V, Filhol O, Nueda A, Gerber D, Benitez MJ, Cochet C: Visualization and molecular analysis of nuclear import of protein kinase CK2 subunits in living cells. *Mol Cell Biochem* 227: 81–90, 2001
12. Martel V, Filhol O, Nueda A, Cochet C: Dynamic localization/association of protein kinase CK2 subunits in living cells: a role in its cellular regulation? *Ann N Y Acad Sci* 973: 272–277, 2002
13. Chantalat L, Leroy D, Filhol O, Nueda A, Benitez MJ, Chambaz EM, Cochet C, Dideberg O: Crystal structure of the human protein kinase CK2 regulatory subunit reveals its zinc finger-mediated dimerization. *EMBO J* 18: 2930–2940, 1999
14. Niefind K, Guerra B, Ermakowa I, Issinger OG: Crystal structure of human protein kinase CK2: Insights into basic properties of the CK2 holoenzyme. *EMBO J* 20: 5320–5331, 2001
15. Glover CV: A filamentous form of *Drosophila* casein kinase II. *J Biol Chem* 261: 14349–14354, 1986
16. Valero E, De Bonis S, Filhol O, Wade RH, Langowski J, Chambaz EM, Cochet C: Quaternary structure of casein kinase 2. Characterization of multiple oligomeric states and relation with its catalytic activity. *J Biol Chem* 270: 8345–8352, 1995